COMMUNICATION

Graphene/MoS_2 Heterostructures for Ultrasensitive Detection of DNA Hybridisation

Phan Thi Kim Loan, Wenjing Zhang, Cheng-Te Lin, Kung-Hwa Wei, Lain-Jong Li,* and Chang-Hsiao Chen**

Ultrasensitive detection of specific DNA or peptide sequences is of great importance in disease diagnostics, environmental monitoring, gene therapy, biomolecular analysis and other biomedical applications.[1–3] Polymerase chain reaction (PCR)[4] and rolling circle amplification (RCA)[5] have been widely used for target and signal amplification. Nevertheless, these methods involve complicated, high cost or time-consuming procedures. Due to the strong demands of rapid, selective and sensitive detection of DNA, optical and electrochemical detection methods relying on the fluorescent or electrochemical tags have been widely used.[6–9] Another approach such as label-free electrical detection has also recently attracted extensive research efforts since no fluorescent or electrochemical tags are required,[10–13] which substantially lowers the cost of the detection. Meanwhile, many new technologies are being developed to enhance the detection sensitivity of DNA concentration. The Si-nanowire sensors based on surface-enhanced Raman scattering[14] or field-effect transistor[15–18] have been demonstrated to detect the DNA at a concentration range of 0.1~1 fM. Several reports have recently made advances to approach the detection limit of sub-femtomolar level.[19–21] An even higher sensitivity in the attomolar range can only be achieved with the aid of signal amplifications.[22] Hence, it is of great challenge to demonstrate the label free and direct attomolar detection.

The large surface area and unique optical/electrical properties of two-dimensionality (2d) monolayer materials make them suitable to interface with biomolecules. For example, graphene is a highly biocompatible and stable material in aqueous solutions.[23] Graphene and its derivatives graphene oxide have been used to interact with DNA molecules for sensitive detection of DNA hybridization,[24–28] where the DNA molecules are found to act as potential gating agents that impose *p*-doping[29] to graphene layers, leading to the changes in the electrical properties of graphene. In principle, the electrical conduction of an ideal graphene with a Fermi level close to the Dirac point is very sensitive to the external charge perturbation. The detection of single molecule has also been successfully demonstrated in gas phase.[30,31] However, the practical biomolecular detection is performed in an aqueous solution, where the water molecules easily affect the Fermi level of graphene such that it is away from the Dirac point. Thus, the reported detection sensitivity for DNA based on the change of graphene properties such as electrical conductivity and carrier concentration has only reached the concentration level of few tens pM.[32] In addition, graphene is known as a material without an energy gap, making it hard to perform the detection with optical absorption or emission methods.

Recently, Zhu et al. have reported that a single-layer MoS_2 nanosheet exhibits high fluorescence quenching ability, which assists the detection of biomolecules with fluorescence probes.[33] Mak et al. have reported that the photoluminescence (PL) intensity of MoS_2 monolayer depends strongly on the applied gate voltage.[34] The ultrasensitivity of the MoS_2 monolayer to the extrinsic charge doping actually provides an excellent avenue for detecting the target DNA molecules, under the condition that DNA molecules need to be dissolved in an aqueous buffer solution. One immediate challenge of using these 2d MoS_2 monolayers for detection is that their optical or electrical property is affected by the presence of moisture and oxygen,[35] which makes it hard to differentiate the signals resulting from DNA and water molecules. Also the MoS_2 film may be degraded or oxidized after exposing to the ambient environment. Here, we report that a hetero-structural stacking film "graphene on MoS_2" (graphene/MoS_2) provides an excellent and ultrasensitive platform for the detection of DNA hybridization. The graphene serves as a protection layer to prevent the reaction between MoS_2 and the ambient environment as well as a biocompatible interface layer to host DNA molecules on its surfaces. The photoluminescence (PL) intensity of the MoS_2 layer in the graphene/MoS_2 stack increases with the concentration of the added target DNA. The detection limit is able to reach the level of aM. The response time for the real time detection in aqueous solutions is as fast as a few minutes, demonstrating that the heterostructures are directly applicable to ultrasensitive detection of DNA detection. The principle revealed in this report also enable the further extension to the detection of antibody-antigen and other probe-target systems.

Dr. W. Zhang, Dr. C.-T. Lin, Dr. L.-J. Li, Dr. C.-H. Chen
Institute of Atomic and Molecular Sciences
Academia Sinica
Taipei 10617, Taiwan
Fax: (+886) 223668264
E-mail: lanceli@gate.sinica.edu.tw;
d9535809@oz.nthu.edu.tw
P. T. K. Loan, Dr. K.-H. Wei
Department of Materials Science & Engineering
National Chiao Tung University
HsinChu 30010, Taiwan
E-mail: khwei@mail.nctu.edu.tw
Dr. L.-J. Li
Department of Medical Research
China Medical University Hospital
Taichung, Taiwan

DOI: 10.1002/adma.201401084

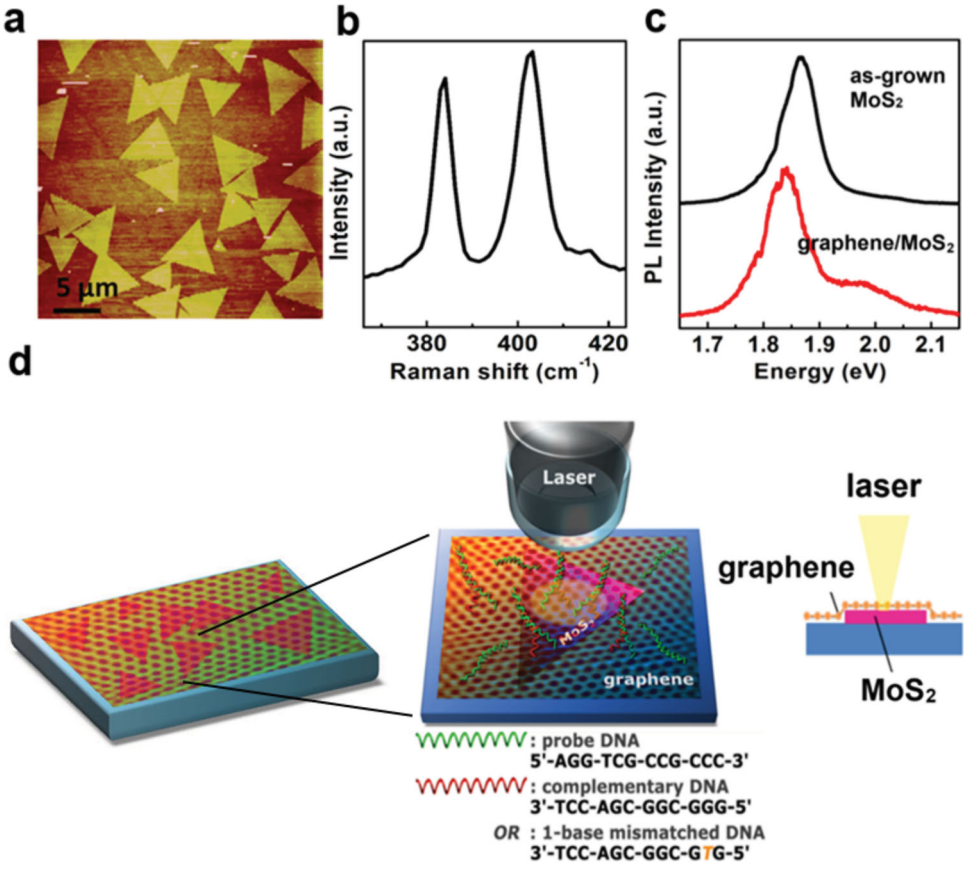

Figure 1. (a) AFM image of a MoS_2 monolayer flake grown at 650 °C on a sapphire substrate. (b) The Raman spectrum for the CVD MoS_2 monolayer. (c) The photoluminescence spectra for the CVD MoS_2 monolayer and graphene/MoS_2 heterostructure. (d) Schematic illustration of the DNA detection method using a microscope and the graphene/MoS_2 heterostructure sensor.

We performed the direct growth of crystalline MoS_2 monolayer flakes on a sapphire substrate by the vapour-phase reaction of MoO_3 and S powders in a hot-wall CVD system.[36,37] The atomic force microscopy (AFM) image in **Figure 1**a shows that the as-grown MoS_2 flakes are mostly monolayers (thickness ~0.72 nm, Figure S1) and approximately several micron in lateral size. Large-area CVD graphene monolayer was grown on copper foils at 1000 °C by a CVD method using a mixture of methane and hydrogen gases as reported elsewhere.[38–40] Figure S2 schematically demonstrates fabrication process of the heterostructure sensor. Figure 1b displays that the as-grown MoS_2 flakes exhibit two characteristic peaks including E′ (or E^1_{2g}) at 384.1 cm^{-1} and A′$_1$ (or A_{1g}) at 402.3 cm^{-1},[41,42] confirming that they are MoS_2 monolayers.[43] To stack the graphene monolayer on MoS_2, a layer of PMMA thin film was coated on the graphene/Cu foil as a transfer supporting layer.[44,45] After the wet etching by a Cu etching solution, the PMMA-supported graphene film was transferred on top of the MoS_2 flakes, followed by the removal of PMMA. The PL spectrum of an as-grown MoS_2 monolayer flake in Figure 1c shows one pronounced emission peak at 1.87 eV, assigned as the A direct excitonic transition.[46] This peak shifts to a lower energy ~1.84 eV after the MoS_2 monolayer was covered with CVD graphene. Note that the PL spectra were scaled for better comparison. Meanwhile, the broad peak at ~1.97 eV belonging to the B direct transition is not pronounced for both as-grown and graphene/MoS_2 structure, likely due to that it is not the lowest energy transition.[47,48]

Figure 1d shows the schematic for the PL measurement of the stacked graphene/MoS_2 film, where a confocal system equipped with a 473 nm laser is used for probing the PL signal of the heterostructures. The sequences of the DNA molecules used in this study are shown in Figure 1d. The integrated PL peak area mappings (laser spot focused to ~1 μm in diameter) were collected before and after the probe DNA immobilization, and after the addition of the DNA analyte solutions (complementary or one-base mismatched DNA) with various concentrations. We perform the PL measurements for the heterostructural stacks in a dry state, where the sample was rinsed with deionized water and dried after each probe DNA immobilization and target DNA addition. It is noted that the methodology of dry state testing has been widely used in many DNA sensing reports,[1,49] where the key step is to immobilize the probe-DNAs on top of graphene by the partial charge transfer of electron from the NH_2 groups of DNA bases to graphene. The target DNAs can be securely bonded to the probe-DNAs and remained on substrate even with violent rinsing while the mismatched-DNAs can be easily removed by rinsing. **Figure 2**a shows the spatial PL mappings for the graphene/MoS_2 stack film immobilized with the probe DNA solution (40 μL; 10

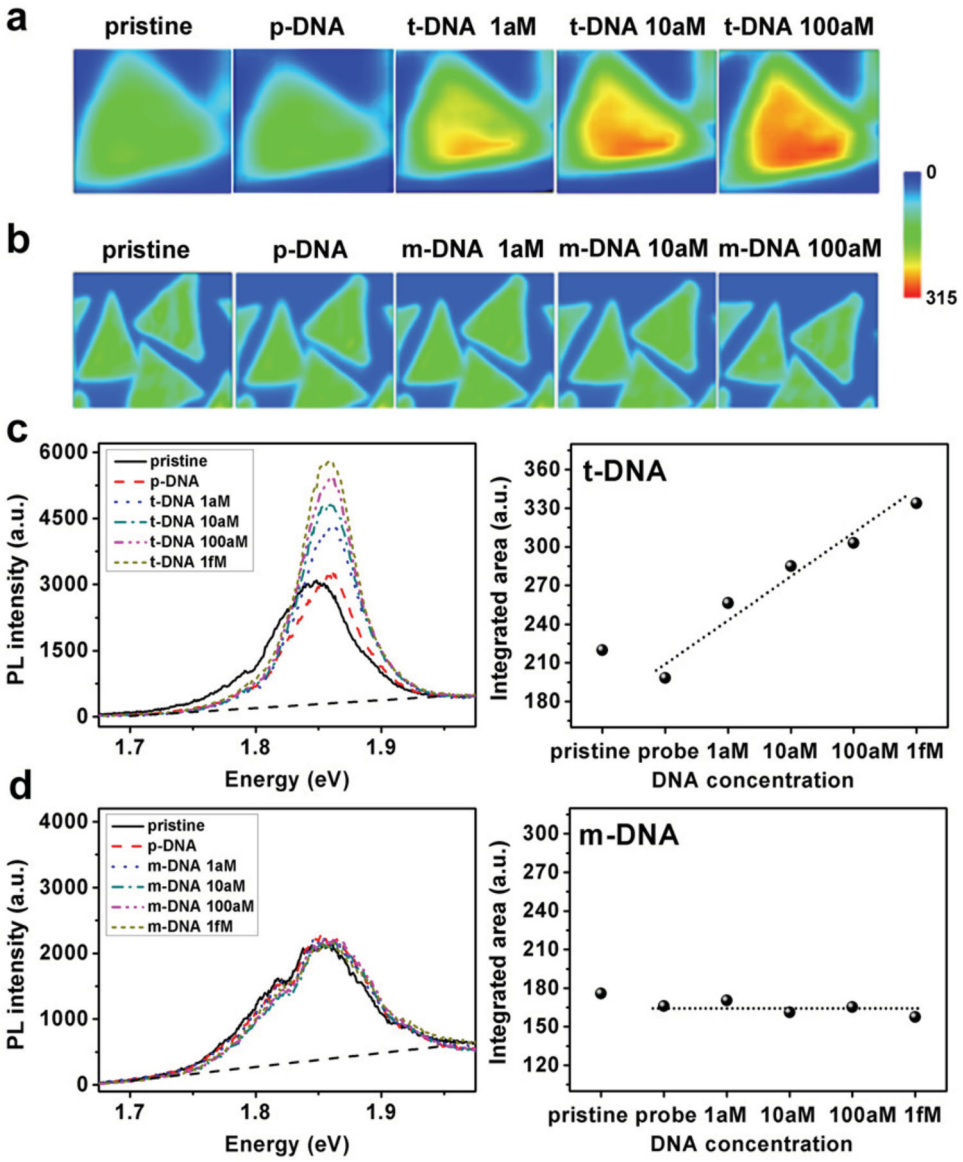

Figure 2. PL peak area mappings of the graphene/MoS_2 heterostructure hybridized with (a) the complementary target DNA and (b) the mismatched DNA. The PL spectra and integrated PL peak area in the presence of (c) target DNA (1, 10, 100, and 1000 aM) and (d) mismatched DNA (1, 10, 100, and 1000 aM).

μM) and hybridized with the complementary DNA solutions (40 μL with various concentrations from 1 aM to 100 aM), where the integrated peak area from 1.7 eV to 1.95 eV (linear baseline is applied in between 1.7 eV and 1.95 eV as shown in the graph) is plotted as the false color based on the color index on the right. Figure S3 shows other sets of PL mappings for the heterostructures hybridized with the complementary target DNA. The bottom graphs in Figure 2b displays the comparative results using one-base mismatched DNAs for hybridization. The PL color mapping clearly and qualitatively reveals that the integrated PL peak area of the graphene/MoS_2 stacks responds to the target DNA but not to the mismatched DNA, demonstrating the capability to differentiate these DNA molecules. To quantitatively analyse the data, we select the site with the highest integrated PL peak area in each mapping and plot them in Figure 2c. The PL of the graphene/MoS_2 stack film with a similar profile to that of pure a MoS_2 film is still originated from the emission of MoS_2[50] and its intensity increases after the immobilization of complementary DNA. More importantly, the integrated PL peak area significantly increases with the concentration of the added complementary DNA solutions. The integrated PL peak area over 1.7 eV to 1.95 eV for each condition is also summarized in Figure 2c, where we can see a positive correlation between integrated PL peak area (in an arbitrary unit) and the concentration of the added complementary DNA from 1 aM to 1 fM. By contrast, when the one-base mismatched DNA solution is used for hybridization, there is no pronounced PL-DNA concentration correlation as shown in Figure 2d. It is already known from previous reports[32,51] the difference between these two hybridization processes (target and one-base

mismatched) is caused by the fact that the target DNA molecules can strongly bind to the probe-DNA and thus stay on the surface of graphene. Hence, the PL intensity is related to the charges of the target DNA molecules and those associated to the target-DNA molecules. These charges are able to build an electric field that affects the charge states of the MoS_2.

It should be noted we have shown in our previous study[32] that the immobilization of probe DNA onto the pristine graphene does not necessarily cause a consistent n- or p-doping since the property of pristine graphene is strongly related to graphene/solution interface properties, which are complicated by the surface condition of graphene, adsorption of DNA and counter ions on graphene, the screening of DNA charges by counter ions, as well as the morphology of single-stranded and hybridized DNAs. However, the subsequent immobilization by addition of complementary DNA always causes a consistent change in electrical properties which can be used for DNA detection.

To further examine whether the PL of the graphene/MoS_2 stacks can be affected by an external electrical field, we perform the PL measurements for a graphene/MoS_2 stacked film under various applied bottom gate voltages (–50 V, –30 V, –10 V, 10 V, 30 V and 50 V). **Figure 3**a shows that each PL profile can be fitted with two Lorentzian peaks at 1.82 eV and 1.86 eV. The trion (A^-) and exciton (A) PL peaks have been identified in the mechanically exfoliated MoS_2 monolayer,[34] where the PL peak caused by a A^- trion is with a lower energy and shows little gate voltage dependence. In contrast, the PL intensity of the higher energy A exciton peak decreases with the increasing positive value of the applied gate voltage since the doping induces the spectral weight reduction of the A excition resonance.[34] Figure 3b displays the integrated peak area for the two fitted PL peaks of the graphene/MoS_2 stack film as a function of the applied gate voltage, where the gate dependence of these two peaks at 1.82 eV and 1.86 eV behaves similarly to the MoS_2 monolayer A^- trion and A exciton peaks, respectively. Since the electrical field is coupled through a thick silicon oxide (300 nm) in this experiment, only limited electrical field is applied to the sample. However, the observed behaviour is consistent with the literature.[34] These observations suggest that the applied electrical field does affect A exciton and thus the overall PL intensity from the MoS_2 in the graphene/MoS_2 stack film. The intensity increases upon the target DNA hybridisation (as displayed in Figure 2) resembles the application of a negative gate voltage, owing to the fact that the target DNA molecules bring negative charges onto the surfaces of the graphene/MoS_2 bilayer. And this conclusion is rational since DNA molecules are with large amounts of negative phosphate groups.

We have previously reported that when a monolayer graphene is stacked onto a MoS_2 monolayer the graphene receives electrons from MoS_2, which reduces the electron concentrations of the initially *n*-doped MoS_2 monolayer.[50] Based on the doping (or gate-voltage) dependence of the A^- exciton PL intensity,[34] the sensitivity is higher when the MoS_2 becomes less *n*-doped (or approaches neutrality). Hence, the incorporation of the graphene not only helps to interface DNA molecules with the MoS_2 layer but also lower the n-doping in MoS_2 layer, making the charge detection more sensitive.

It has been reported that the peak width and position of Raman A'_1 band (~402 cm^{-1}) are sensitive to the Fermi energy change or carrier concentration in MoS_2.[52] To understand the details of the PL enhancement upon DNA hybridisation (i.e. additional doping induced by DNA adsorption on graphene/MoS_2), Raman spectroscopy is adopted to monitor the change of the charge state in MoS_2 monolayers. Since a low probe-DNA concentration did not result in apparent changes in Raman features, we perform the hybridisation with much higher target-DNA concentrations in the range from 1 pM to 1 nM, where the baseline corrected Raman spectra are shown in Figure S4. When the Raman spectra are normalized to the E' peak height, both the peak intensity and peak energy of A'_1 increase with the target-DNA concentrations. The A'_1 frequency shows a blue-shift from ~402.1 to ~404.7 cm^{-1} as the target-DNA concentration increases, while the E' frequency is fixed at ~384.1 cm^{-1}. The frequency separation between the A'_1 and E' increases from 18 to 20.6 cm^{-1}. These results show that the A'_1 vibration mode is very sensitive to the charge doping, and the E' mode remains relatively inert. Meanwhile, the peak width becomes narrower with the DNA concentration, indicating that the MoS_2 layer becomes less *n*-doped (or reduction in electron concentration).[52]

It is interesting to know whether the graphene layer is affected by the DNA sensing. Figure S5 shows the Raman D and G band profiles for the graphene directly on top of

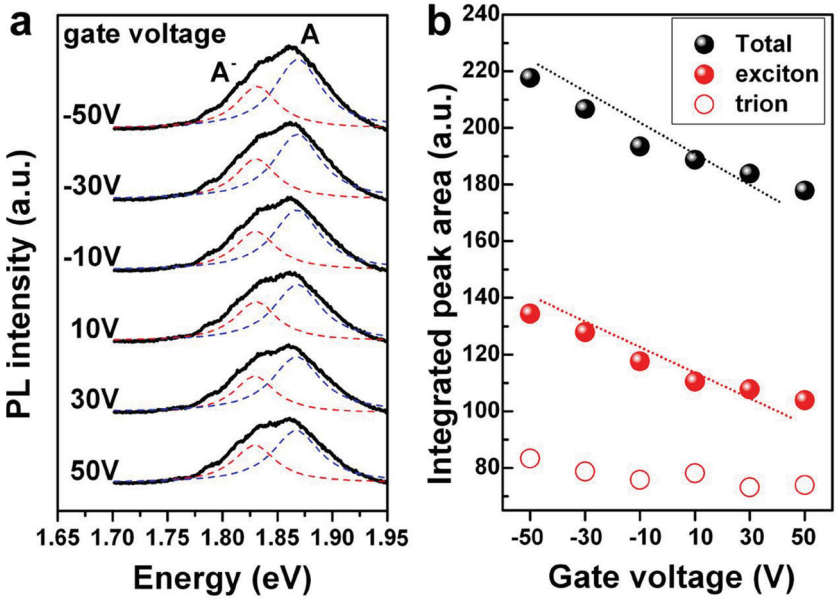

Figure 3. (a) The photoluminescence spectra of a graphene/MoS_2 field effect transistor in the range of 1.7–1.95 eV for the indicated back-gate voltages. The A^- trion and A exciton features are fitted to two Lorentzian peaks (dashed lines). The A^- trion (red dashed line) and A exciton (blue dashed line) intensity responds differently with the gate voltage. (b) Gate voltage dependence of the integrated PL peak area for the A^- trion and A exciton peaks.

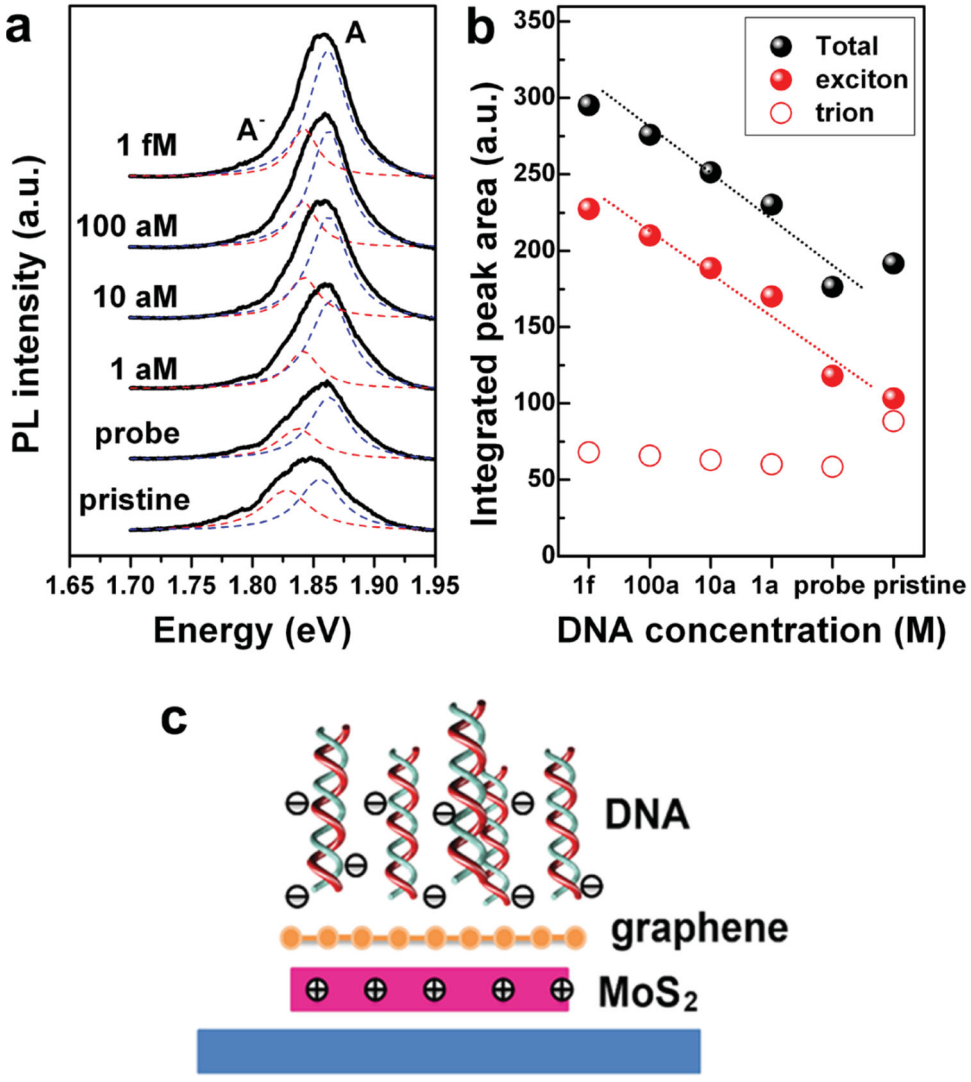

Figure 4. (a) The photoluminescence spectra of a graphene/MoS_2 stacked film in the range of 1.7–1.95 eV. The PL peak area of the A^- trion (red dashed line) and A exciton (blue dashed line) responds differently with target DNA concentration. (b) Dependence of the integrated PL peak area on target DNA concentration. (c) Schematic illustration for the charge distribution of DNA on graphene/MoS_2.

the MoS_2 flake. It is observed that the G and D bands do not change at all with the hybridisation process, suggesting that the Fermi energy of graphene layer is not influenced by the DNA sensing. This may be understood by the preferred electron transfer from MoS_2 to graphene caused by the band offset between MoS_2 and graphene.[50] In another word, any induced hole in graphene shall be filled by the electron from MoS_2, leading to the reduction of electrons in MoS_2 layer.

The PL spectra for the graphene/MoS_2 stacks added with various concentrations of target DNA are shown in **Figure 4**a. To simplify the peak fitting, a line connecting the data point at 1.7 eV and at 1.95 eV is used as the baseline for each PL spectrum. Similar to Figure 3, Figure 4a shows that each PL profile can be fitted to two Lorentzian peaks attributed to the A^- trion and A exciton peaks. The change of the peak intensity with the target DNA concentration is shown in Figure 4b. The PL intensity of the A exciton is much more sensitive to the target DNA concentration than the A^- trion. Based on the conclusion drawn from Figure 3, the amount of the positive charges in MoS_2 film increase with the addition of target DNA. Figure 4c schematically illustrates that the DNA adsorption on graphene/MoS_2 results in more positive charges in the MoS_2 and thus enhances it's overall PL intensity.

The above results and discussions show that the detection of DNA molecules with the photoluminescence from the graphene/MoS_2 heterostructure is feasible. For more practical application, it is useful to be able to perform the real time and ultra-sensitive detection in aqueous states. **Figure 5** shows the real time measurement of the PL intensity for the probe-DNA immobilized graphene/MoS_2 structures in a DNA buffer solution as well as the solutions incorporating various concentrations of DNA molecules (1a M, 10 aM, 100 aM 1f M) at the time indicated in the figure. The fast increase in PL intensity after each solution replacement suggests the occurrence of DNA hybridisation. More importantly, the proposed graphene/MoS_2 heterostructure is able to sense the aM

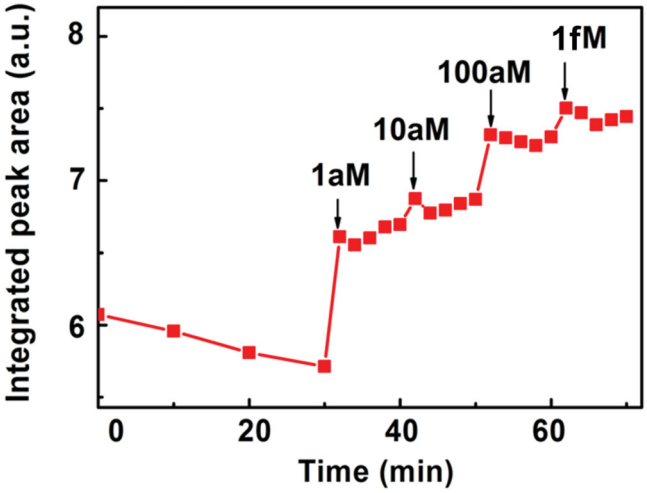

Figure 5. The real-time photoluminescence response of the graphene/MoS_2 to the target-DNA with increased concentration.

concentration of target DNA. More data set is shown in supporting Figure S6.

In summary, we have devised a graphene/MoS_2 heterostructure by stacking graphene on a CVD MoS_2 crystalline monolayer, and the photoluminescence characteristics of the constructed graphene/MoS_2 film are used for label-free and selective detection of DNA hybridization. The graphene serves as a protection layer to prevent the reaction between MoS_2 and the ambient environment as well as a biocompatible interface layer to host DNA molecules on its surfaces. The photoluminescence (PL) intensity of the MoS_2 layer in the graphene/MoS_2 stack increases with the concentration of the added target DNA. The differentiation of complementary and one-base mismatched DNA with the graphene/MoS_2 heterostructure can be performed at a concentration as low as 1 aM (10^{-18} M), indicating high sensitivity for this proof-of-concept heterostucture. It is anticipated that the graphene/MoS_2 heterostructure may be further expanded to the area of label-free detection of protein, metal-ion contaminants in water, bacteria, and intercellular or extracellular activities.

Experimental Section

CVD Growth of MoS_2: MoS_2 triangular single crystals were synthesized based on our previous work.[53] In brief, sapphire (0001) substrate (Tera Xtal Technology Corp) were first cleaned in a H_2SO_4/H_2O_2 (70:30) solution heated at 100 °C for 1 hr. The substrates were placed in the center of a 4" tubular furnace on a quartz holder tilted 60° to tube horizontal. Precursors of 0.6 g MoO_3 (Sigma-Aldrich, 99.5%) in Al_2O_3 crucible was placed 12 cm away from substrates and S (Sigma-Aldrich, 99.5%) powder in quartz tube was placed 8 cm away from furnace open-end at upstream position in a 4" quartz tube. The furnace was first heated to 150 °C at 10 °C/min rate with 70 sccm Ar at 10 torr and annealed for 20 minutes, then reached 650 °C at 25 °C/min rate and kept for 1 hr. Sulfur was heated by heating belt at 160 °C when furnace reached 400 °C. After growth, furnace was slowly cooled to room temperature.

CVD Growth of Graphene: The CVD growth of graphene was performed in a furnace (TF555500030, Lindberg/Blue M) with a quartz tube (diameter 25 mm). A copper (Cu) foil (Alfa Aesar, item No.13382, thickness 25 μm, purity 99.8%) was loaded into the center of the tube, the system was flushed with a constant flow of argon/hydrogen (200/20 sccm) at 800 Torr for 30 min, and both gas flows were maintained through the remaining process. The Cu foil was annealed at 1050 °C for 60 min to remove organic matter and oxides from the surface. After the annealing process, a gas mixture of methane, hydrogen and argon (CH_4 = 3 sccm, H_2 = 1 sccm, Ar = 500 sccm at 800 Torr) was introduced for 10 min for graphene growth. After the growth of graphene, the graphene/Cu foil was cooled to 25 °C.

Fabrication of Graphene/MoS_2 Devices: To transfer the as-grown graphene onto the MoS_2 monolayer, the graphene/Cu foil (size 15 mm × 15 mm) was spin-coated with a thin layer of PMMA (MicroChem Co., NANO PMMA 950K A4) to protect the graphene film, followed by baking at 100 °C for 1 min. The samples were immersed in a solution of ammonium persulfate (0.1 M; J. T. Baker, ACS reagent) at 25 °C. The Cu foil was etched away over 3 h. The PMMA-supported graphene was transferred into a Petri dish containing a copious amount of distilled water for 2 hour to dilute and remove the etchant and residues. The PMMA-supported graphene layer was then transferred on to the MoS_2 monolayer and dried on a hot plate at 70 °C for 30 min. Finally, the PMMA was removed by acetone (J. T. Baker, CMOS Grade) at 25 °C for 2 hour, and then the sample was rinsed with isopropyl alcohol (J. T. Baker, CMOS Grade) and distilled water to complete the transfer process.

Immobilization of DNAs on Graphene/MoS_2: The single-strain sequence of probe, complementary, and one-base mismatched DNAs (Sigma Aldrich) we used are presented below: probe) 5′-AGG-TCG-CCG-CCC-3′; complementary) 3′-TCC-AGC-GGC-GGG-5′; one-base mismatched) 3′-TCC-AGC-GGC-GTG-5′. The assigned concentrations of complementary and one-base mismatched DNAs were prepared by diluting them with 1× PBS solvent (phosphate-buffered saline; UniRegion Bio-Tech). 1× PBS is composed of 13.7 mM NaCl, 0.27 mM KCl, 0.43 mM Na_2HPO_4, and 0.147 mM KH_2PO_4. For the graphene/MoS_2 sensor device, the exposed surface area of the stack film to DNA solutions is 0.25 cm^2, chosen based on our micro PL set-up. The quantity of DNA solution (40 μL) is enough to cover the exposed surfaces of the stacked films. First, the graphene/MoS_2 device was immobilized in 10 μM probe DNA for 4 h at room temperature. A following rinsing step with DI water was carried out to remove weakly-bound DNAs. The complementary or one-base mismatched DNAs were dropped onto the device in sequence from 1 aM to 1000 aM for hybridization with probe DNA. It took 2 hours for hybridization at each concentration and after that the rinsing step was always done. A full hybridization experiment was accomplished as a control study by mixing probe and complementary DNAs in 1× PBS for several hours, and the mixture was then immobilized onto the device for 2 h, followed by a standard washing process.

Measurements and Characterizations: The bottom-gated graphene/MoS_2/SiO_2 FETs were measured in a semiconductor parameter analyser (Keithley 4200-SCS). Photoluminescence and Raman spectra were collected in NT-MDT confocal Raman microscopic system (laser wavelength: 473 nm; laser power: 1 mW; spot size: ≈ 1 μm). The spectra taken from samples were calibrated against a Si peak at 520 cm^{-1}.

Supporting Information

Supporting Information is available from the Wiley Online Library or from the author.

Acknowledgements

This research was supported by Academia Sinica (IAMS and Nano program) and National Science Council Taiwan (NSC-102–2119-M-001–005-MY3).

Received: March 10, 2014
Revised: April 14, 2014
Published online: May 19, 2014

[1] F. Wei, P. B. Lillehoj, C.-M. Ho, *Pediatr. Res.* **2010**, *67*, 458.
[2] D. Li, S. Song, C. Fan, *Acc. Chem. Res.* **2010**, *43*, 631.
[3] A. L. Beaudet, J. W. Belmont, *Annu. Rev. Med.* **2008**, *59*, 113.
[4] S. Yang, R. E. Rothman, *Lancet Infect. Dis.* **2004**, *4*, 337.
[5] V. V. Demidov, *Expert Rev. Mol. Diagn.* **2002**, *2*, 542.
[6] F. Lu, L. Gu, M. J. Meziani, X. Wang, P. G. Luo, L. M. Veca, L. Cao, Y.-P. Sun, *Adv. Mater.* **2009**, *21*, 139.
[7] D. Fu, H. Lim, Y. Shi, X. Dong, S. G. Mhaisalkar, Y. Chen, S. Moochhala, L.-J. Li, *J. Phys. Chem. C* **2008**, *112*, 650.
[8] X. Tang, S. Bansaruntip, N. Nakayama, E. Yenilmez, Y.-l. Chang, Q. Wang, *Nano Lett.* **2006**, *6*, 1632.
[9] J. Wang, *Electroanalysis* **2005**, *17*, 7.
[10] S. Sorgenfrei, C.-y. Chiu, R. L. Gonzalez, Y.-J. Yu, P. Kim, C. Nuckolls, K. L. Shepard, *Nat. Nanotechnol.* **2011**, *6*, 126.
[11] E. L. Gui, L.-J. Li, K. Zhang, Y. Xu, X. Dong, X. Ho, P. S. Lee, J. Kasim, Z. X. Shen, J. A. Rogers, S. G. Mhaisalkar, *J. Am. Chem. Soc.* **2007**, *129*, 14427.
[12] K. Maehashi, T. Katsura, K. Kerman, Y. Takamura, K. Matsumoto, E. Tamiya, *Anal. Chem.* **2006**, *79*, 782.
[13] E.-L. Gui, L.-J. Li, P. S. Lee, A. Lohani, S. G. Mhaisalkar, Q. Cao, S. J. Kang, J. A. Rogers, N. C. Tansil, Z. Gao, *Appl. Phys. Lett.* **2006**, 89.
[14] Z. Y. Jiang, X. X. Jiang, S. Su, X. P. Wei, S. T. Lee, Y. He, *Appl. Phys. Lett.* **2012**, 100.
[15] N. Lu, A. Gao, P. Dai, T. Li, Y. Wang, X. Gao, S. Song, C. Fan, Y. Wang, *Nat. Methods* **2013**, *63*, 212.
[16] A. Gao, N. Lu, Y. Wang, P. Dai, T. Li, X. Gao, Y. Wang, C. Fan, *Nano Lett.* **2012**, *12*, 5262.
[17] A. Gao, N. Lu, P. Dai, T. Li, H. Pei, X. Gao, Y. Gong, Y. Wang, C. Fan, *Nano Lett.* **2011**, *11*, 3974.
[18] J.-J. Xu, W.-W. Zhao, S. Song, C. Fan, H.-Y. Chen, *Chem. Soc. Rev.* **2014**, *43*, 1601.
[19] Y. Yan, W. Sha, J. Sun, X. Shu, S. Sun, J. Zhu, *Chem. Commun.* **2011**, *47*, 7470.
[20] X. Zhou, S. Xia, Z. Lu, Y. Tian, Y. Yan, J. Zhu, *J. Am. Chem. Soc.* **2010**, *132*, 6932.
[21] S. Pinijsuwan, P. Rijiravanich, M. Somasundrum, W. Surareungchai, *Adv. Eng. Mater.* **2010**, *12*, B649.
[22] Y. Wen, H. Pei, Y. Shen, J. Xi, M. Lin, N. Lu, X. Shen, J. Li, C. Fan, *Sci. Rep.* **2012**, 2.
[23] C.-H. Chen, C.-T. Lin, W.-L. Hsu, Y.-C. Chang, S.-R. Yeh, L.-J. Li, D.-J. Yao, *Nanomed. Nanotechnol. Biol. Med.* **2013**, *9*, 600.
[24] Z. Yin, S. Sun, T. Salim, S. Wu, X. Huang, Q. He, Y. M. Lam, H. Zhang, *ACS Nano* **2010**, *4*, 5263.
[25] C.-Y. Su, Y. Xu, W. Zhang, J. Zhao, X. Tang, C.-H. Tsai, L.-J. Li, *Chem. Mater.* **2009**, *21*, 5674.
[26] G. Eda, G. Fanchini, M. Chhowalla, *Nat. Nanotechnol.* **2008**, *3*, 270.
[27] L. J. Cote, F. Kim, J. Huang, *J. Am. Chem. Soc.* **2008**, *131*, 1043.
[28] P. K. Ang, W. Chen, A. T. S. Wee, K. P. Loh, *J. Am. Chem. Soc.* **2008**, *130*, 14392.
[29] N. Mohanty, V. Berry, *Nano Lett.* **2008**, *8*, 4469.
[30] Y.-H. Zhang, Y.-B. Chen, K.-G. Zhou, C.-H. Liu, J. Zeng, H.-L. Zhang, Y. Peng, *Nanotechnology* **2009**, *20*, 185504.
[31] F. Schedin, A. K. Geim, S. V. Morozov, E. W. Hill, P. Blake, M. I. Katsnelson, K. S. Novoselov, *Nat. Mater.* **2007**, *6*, 652.
[32] C.-T. Lin, P. T. K. Loan, T.-Y. Chen, K.-K. Liu, C.-H. Chen, K.-H. Wei, L.-J. Li, *Adv. Funct. Mater.* **2013**, *23*, 2301.
[33] C. Zhu, Z. Zeng, H. Li, F. Li, C. Fan, H. Zhang, *J. Am. Chem. Soc.* **2013**, *135*, 5998.
[34] K. F. Mak, K. He, C. Lee, G. H. Lee, J. Hone, T. F. Heinz, J. Shan, *Nat. Mater.* **2013**, *12*, 207.
[35] S. Tongay, J. Zhou, C. Ataca, J. Liu, J. S. Kang, T. S. Matthews, L. You, J. Li, J. C. Grossman, J. Wu, *Nano Lett.* **2013**, *13*, 2831.
[36] Y.-H. Lee, L. Yu, H. Wang, W. Fang, X. Ling, Y. Shi, C.-T. Lin, J.-K. Huang, M.-T. Chang, C.-S. Chang, M. Dresselhaus, T. Palacios, L.-J. Li, J. Kong, *Nano Lett.* **2013**, *13*, 1852.
[37] Y.-C. Lin, N. Lu, N. Perea-Lopez, J. Li, Z. Lin, X. Peng, C. H. Lee, C. Sun, L. Calderin, P. N. Browning, M. S. Bresnehan, M. J. Kim, T. S. Mayer, M. Terrones, J. A. Robinson, *ACS Nano* **2014** DOI: 10.1021/nn5003858.
[38] C.-H. Chen, C.-T. Lin, Y.-H. Lee, K.-K. Liu, C.-Y. Su, W. Zhang, L.-J. Li, *Small* **2012**, *8*, 43.
[39] C.-Y. Su, D. Fu, A.-Y. Lu, K.-K. Liu, Y. Xu, Z.-Y. Juang, L.-J. Li, *Nanotechnology* **2011**, *22*, 185309.
[40] S. Bae, H. Kim, Y. Lee, X. Xu, J.-S. Park, Y. Zheng, J. Balakrishnan, T. Lei, H. Ri Kim, Y. I. Song, Y.-J. Kim, K. S. Kim, B. Ozyilmaz, J.-H. Ahn, B. H. Hong, S. Iijima, *Nat. Nanotechnol.* **2010**, *5*, 574.
[41] Y. Zhan, Z. Liu, S. Najmaei, P. M. Ajayan, J. Lou, *Small* **2012**, *8*, 966.
[42] H. Terrones, E. D. Corro, S. Feng, J. M. Poumirol, D. Rhodes, D. Smirnov, N. R. Pradhan, Z. Lin, M. A. T. Nguyen, A. L. Elias, T. E. Mallouk, L. Balicas, M. A. Pimenta, M. Terrones, *Sci. Rep.* **2014**, *4*, 4215.
[43] Y. Yu, C. Li, Y. Liu, L. Su, Y. Zhang, L. Cao, *Sci. Rep.* **2013**, 3.
[44] C.-L. Hsu, C.-T. Lin, J.-H. Huang, C.-W. Chu, K.-H. Wei, L.-J. Li, *ACS Nano* **2012**, *6*, 5031.
[45] C.-Y. Su, A.-Y. Lu, C.-Y. Wu, Y.-T. Li, K.-K. Liu, W. Zhang, S.-Y. Lin, Z.-Y. Juang, Y.-L. Zhong, F.-R. Chen, L.-J. Li, *Nano Lett.* **2011**, *11*, 3612.
[46] A. Splendiani, L. Sun, Y. Zhang, T. Li, J. Kim, C.-Y. Chim, G. Galli, F. Wang, *Nano Lett.* **2010**, *10*, 1271.
[47] S. Wu, C. Huang, G. Aivazian, J. S. Ross, D. H. Cobden, X. Xu, *ACS Nano* **2013**, *7*, 2768.
[48] J. S. Ross, S. Wu, H. Yu, N. J. Ghimire, A. M. Jones, G. Aivazian, J. Yan, D. G. Mandrus, D. Xiao, W. Yao, X. Xu, *Nat. Commun.* **2013**, *4*, 1474.
[49] J. Liu, Z. Cao, Y. Lu, *Chem. Rev.* **2009**, *109*, 1948.
[50] W. Zhang, C.-P. Chuu, J.-K. Huang, C.-H. Chen, M.-L. Tsai, Y.-H. Chang, C.-T. Liang, Y.-Z. Chen, Y.-L. Chueh, J.-H. He, M.-Y. Chou, L.-J. Li, *Sci. Rep.* **2014**, 4.
[51] T.-Y. Chen, P. T. K. Loan, C.-L. Hsu, Y.-H. Lee, J. Tse-Wei Wang, K.-H. Wei, C.-T. Lin, L.-J. Li, *Biosens. Bioelectron.* **2013**, *41*, 103.
[52] B. Chakraborty, A. Bera, D. V. S. Muthu, S. Bhowmick, U. V. Waghmare, A. K. Sood, *Phys. Rev. B* **2012**, *85*, 161403.
[53] Y.-H. Lee, X.-Q. Zhang, W. Zhang, M.-T. Chang, C.-T. Lin, K.-D. Chang, Y.-C. Yu, J. T.-W. Wang, C.-S. Chang, L.-J. Li, T.-W. Lin, *Adv. Mater.* **2012**, *24*, 2320.